Aust. Met. Mag. 32 (1984) 207-226

551.553.11

Colliding sea-breezes and the creation of internal atmospheric bore waves: two-dimensional numerical studies

R. H. Clarke, Meteorology Department, University of Melbourne

(Manuscript received August 1984; revised December 1984)

Gravity currents and bores in the lower atmosphere play an important part in determining mesoscale weather events quite generally. Researches into these phenomena on Cape York Peninsula have shed light on the behaviour of both, in rather quiet and otherwise undisturbed conditions.

The part played by sea-breezes in initiating bores was strongly suggested by field observations, but a decisive demonstration of the exact sequence of events resulting in a bore was not found.

A series of numerical experiments has been carried out, and these have shown clearly what happens when two sea-breeze circulations of different provenance interact. Under conditions commonly prevailing on the Peninsula in October, this collision or interaction of sea-breezes is both observed and found by two-dimensional numerical modelling to occur.

When two sea-breeze fronts collide, or one overtakes the other, cool sea-breeze modified boundary-layer air is forced upward to form a hump of relatively cool air. This process continues until a condition for bore formation is met. At that stage, in general, two bores are formed, moving with approximately the respective velocities of the sea-breeze fronts before collision.

New insight has also been obtained into the behaviour of sea-breeze surges in the tropics, in the presence of clear skies and a coast-normal geostrophic wind. Under suitable conditions, they can be deeper and more powerful than is generally supposed, and can penetrate much further inland in some cases, and in others out to sea. Coast-parallel geostrophic wind components have little effect on this penetration, nor does a hill or escarpment near the coast.

Introduction

Field observations on the north Queensland phenomenon known as the 'morning glory' have established that it is an internal undular bore; that the most commonly occurring variety, coming from the east-northeast, begins its career as a sea-breeze surge originating inland from the east coast of Cape York Peninsula, but that it is transformed into a bore over the Peninsula, usually at a distance of 50 to 100 km inland of the west coast (but occasionally apparently in the Gulf of Carpentaria) within a very few hours of midnight. It propagates towards the west-southwest with a speed of about 10 m s^{-1}, and has been shown at Burketown and Macaroni Station to have associated vertical velocities of the order of 5 m s^{-1}. Radiosonde observations on the Peninsula, and a single pair at Burketown, also suggest that (because of temperature and humidity changes) cooler Pacific Ocean air may penetrate at least to these places (i.e. 650 km) at some time behind the bore, but by then the gravity current is so diffuse that there is nothing to mark its arrival.

On Bureau of Meteorology records, the passage of the bore is remarkable for a sharp pressure jump on the barograph, usually of magnitude 0.5 to 1.5 mb, which shows little or nothing of the post-bore 'embroidery' revealed when better instrumentation is used. Indeed this embroidery sometimes takes the form of large amplitude wavelike oscillations lasting for as long as two hours, with a pronounced tendency for an approximate period of about ten minutes to predominate (see e.g. the pressure record for Karumba on 9 October 1980 in Clarke 1983b). The term embroidery is then inappropriate, but for the majority of observed morning glories the main pressure feature is the jump: furthermore, a bore consisting mainly of waves in one place may subsequently present as mainly a jump at others, as on 10-11 October 1981 (Smith and Morton 1984). Visual observations often reveal a long line of cloud, of height reaching from several hundred metres to one or two kilometres or more, usually smooth, and not uncommonly followed by subsequent lines, not so

smooth and regular, also at intervals of about ten minutes, and up to eight in number.

The bore, with its pressure jump and propagating cloud line is marked at the surface as well by the arrival of a squally wind from the direction from which the bore is coming, maximum wind corresponding to maximum rate of increase of pressure, and lasting several minutes. Changes in surface temperature and humidity are not usually remarkable, and may be in either direction. The maximum speed of the wind, at least at a height of from one to several hundred metres, approaches, and sometimes even surpasses, that of the rate of advance of the bore, but for a very limited time. The wind squall may be followed by others of similar strength and direction, also corresponding to rate of increase of pressure, and accompanying the cloud lines.

These features have been described by Clarke (1972); Neal et al. (1977); Clarke et al. (1981), hereafter referred to as CSR; Smith et al. (1982); Clarke (1983a, 1983b), hereafter referred to as I and II respectively; Egger (1984); Smith and Morton (1984); and Clarke (1985), hereafter referred to as III. In II it was concluded from the observations that the internal undular bores of the Gulf of Carpentaria (hereafter called 'the Gulf') are produced by the interaction of an active gravity current (sea-breeze surge) with the remnants of a weaker sea-breeze, from the other side of Cape York Peninsula (hereafter referred to as 'the Peninsula'). This second sea-breeze preconditions the lower atmosphere to make bore formation more probable.

The author's two-dimensional modelling has recently been supplemented by extensive computations with an improved version of his hydrostatic model. The model was overhauled for greater efficiency and flexibility, and a five point filter was incorporated to cope with the large amplitude two-grid waves resulting from the collision of sea-breezes, as mentioned in II. The objective was to investigate further the behaviour of sea-breezes in the presence of a geostrophic wind, and to demonstrate the creation and subsequent history of bores following a collision of the sea-breezes from both coasts of a 'peninsula' of the dimensions of Cape York. The results are informative, both as to the development of tropical sea-breezes, and the exact manner in which the bore is formed and propagates, following the collision.

The 'single coast' sea-breeze model

The model has been briefly described earlier, in I. Most of the experiments whose results are summarised below have been carried out with solar radiation determined by clear skies (allowance was made for possible condensation, but none occurred), solar elevation for 1 October at latitude 16.7 °S, with the albedo of a dry sclerophyll forest, and soil moisture of 4 mm. Sea surface and ground temperatures at the 4 model levels were set initially to 27 °C, and atmospheric temperature and humidity, uniform horizontally, as measured at Macaroni Station in 1981 (see II). No orography was included in the 'single coast' series, although this had been done earlier, to simulate the Canberra sea-breeze (see I). The model has 30 grid-points in the vertical, the top being at about 50 mb, and a horizontal grid spacing of either 5 or 10 km, in a domain extending both landward and seaward for either 500 or 700 km.

Results with geostrophic* wind onshore ($u_g>0$)

This case has received little attention in the literature (but see Pearson et al. 1983), perhaps because in the near-coastal area there is little evidence of a sea-breeze. Well inland, especially in the tropics, the case may be quite different; for example, with an onshore geostrophic wind of 8 m s^{-1}, a strong sea-breeze surge develops, and with the parameters as assumed is located about 176 km inland at 1600 hr.

Five stages in the development of a sea-breeze may be identified. We concentrate on flat land at low latitudes.

1. The immature or formative stage. As heating over the land progresses, the value of x_s, the inland penetration, increases monotonically with time, while the speed, c_s, of the surge front, although increasing gradually after about 1100 hr†, is maintained at a large fraction of the geostrophic wind, i.e. at some average value of the inland component of the boundary layer wind. The developing front is in a far from steady state, as shown by the isentropes (θ) and relative streamlines (isopleths of ψ) normal to the surge front, in Fig. 1. In Fig. 1(a) the relative flow is **through** the leading isentropes, which are vertical through most of the mixed layer, with upward flow in front and downward behind. The capping inversion near 2700 m is being distorted by the flow. The process which maintains the leading isentropes in a near-vertical position is clearly the convective overturning, which inhibits the formation of the superadiabatic lapse rates which would otherwise be produced by the advection indicated. Downward displacement of isentropes to the rear of the developing surge front is indicated by the streamlines. With a rather large geostrophic wind (12.5 m s^{-1}) the sea-breeze retains some similarity to this early stage, as shown by Fig. 2 for 2045 hr. By this time the surge front has ceased to develop further, has penetrated 386 km inland, and still has a speed c_s less than u_g. Flow through the leading isentropes, as in Fig. 1, is still occurring, and it is still being prevented, by convective overturning, from sloping forward with height. As in Fig. 1, descent behind the leading edge is flattening the isentropes.

* The term 'ambient' in this context is imprecise because of spatial variation; 'geostrophic', with components in both the x and y direction, is to be preferred.

† Henceforth all times are local mean times. When referring to observed data, the times are based on long. 142.5 °E, about the middle of the observing network.

Fig. 1 (a) Isentropes (full lines) and relative streamlines (thin lines) for a sea-breeze front, in a section normal to the coast. x is horizontal distance from the coast, positive inland. The stream function is computed from

$$\psi(x,z) = \int_0^z [\rho(x,z)\,[c_s - u(x,z,)]]\,dz$$

with $\psi(x,O) = O$.

z is the vertical coordinate, ρ density, c_s the speed of the disturbance and u the wind component directed inland. The $\psi = 0$ streamline is indicated; others are at intervals of 1000 kg $m^{-1}\,s^{-1}$. M is streamfunction minimum. Time is 1245 hr; $u_g = 5$ m s^{-1}; $c_s = 4.0$ m s^{-1}; ϕ = latitude = 16.7°S; $z_o = 0.02$ m; date is 1 October; $w_{max} = 0.20$ m s^{-1} at 1120 m.

(b) Same as for (a), but time 1705 hr; $c_s = 6.1$ m s^{-1}; $w_{max} = 0.20$ m s^{-1} at 1475 m.

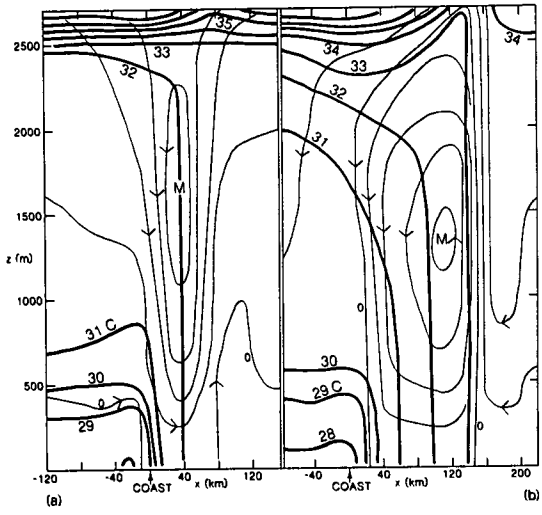

Decreasing the roughness parameter, z_o, from 0.16 to 0.02 m had little effect on the inland penetration of this surge, increasing it, by 2045 hr, by only 44 km.

2. The early mature stage. This is illustrated by Fig. 1(b) for 1705 hr, which shows that the leading isentropes of the sea-breeze surge are nearly parallel with the streamlines over the lowest 2000 m, while elsewhere the isentropes are being depressed by the motion. As in the immature stage, this is certainly not a steady-state gravity current. The maximum value of the inland-directed wind component is 11 m s^{-1} at 220 m, as against a geostrophic wind of 5 m s^{-1}, while $c_s = 6.1$ m s^{-1} now exceeds u_g. Acceleration is occurring, with sunset still about an hour away.

3. Late mature stage. The leading isentropes are still steeply inclined over much of their height, but are being pushed back over their upper portion. All other isentropes have been, and are being, flattened. The stable boundary layer air is being lifted over the top of the sea-breeze. The surge speed (with $u_g = 5$ m s^{-1}) has increased markedly to 10.4 m s^{-1} at 2230

Fig. 2 As for Fig. 1. Time 2045 hr; $u_g = 12.5$ m s^{-1}; $c_s = 10.9$ m s^{-1}; $\phi = 16.0$°S; date 1 July; $z_o = 0.16$m; $w_{max} = 0.09$ m s^{-1} at 1480 m.

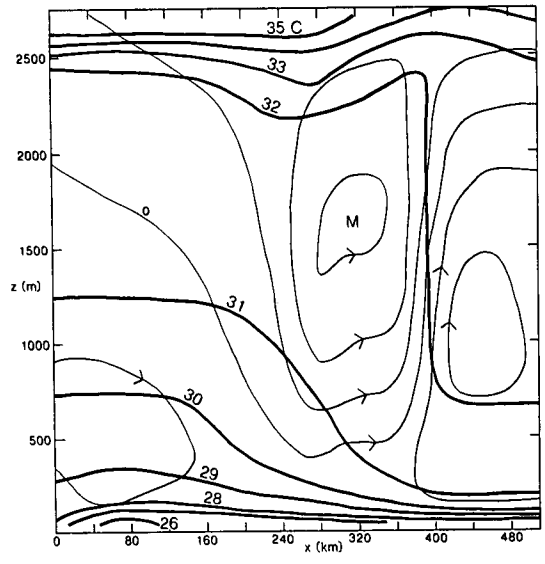

hr, and the maximum value of u (at 220 m) is 14 m s^{-1}. The surge front is still sharp and active. Strong as the circulation is, the upward motion does not extend far above the top of the daytime mixed layer at about 2700 m. The centre of the horizontal vortex comprising the sea-breeze circulation has now shifted to be near its leading edge.

4. Early degenerate stage (see Fig. 3). This is a type of configuration of streamlines and isentropes observed before in surge situations (Clarke 1961; Clarke 1965; Simpson et al. 1977; I). The disturbance is propagating as an unsteady gravity current, resulting from the isobaric (i.e. nearly horizontal) density gradients set up by daytime heating over land. It is driving a cool, flattening wedge under the warm inland air, and in low latitudes, where geostrophic balance is slow to be achieved, this continues throughout the night. The circulation is strongly asymmetrical, maintaining the shape of the leading isentrope in its lowest 1000 m, but depressing all others. The disturbance may be regarded as a degenerate gravity current, a type of finite amplitude, unsteady solitary wave, or as a mesoscale horizontal vortex. It is essentially unsteady, evolving towards a condition of zero isobaric density gradient.

5. Late degenerate stage. This is illustrated in Fig. 18(a). The only marked difference from the previous stage is that there is now no closed circulation near the leading edge of the still recognisable but degenerate gravity current, which may be considered an unsteady long wave followed by a dissipating gravity current. The lower levels of the leading isentropes are still being approximately maintained, but

Fig. 3 As for Fig. 1. Time 0115 hr; $u_g = 5$ m s^{-1}; $c_s = 11.8$ m s^{-1}; $w_{max} = 0.16$ m s^{-1} at 1130 m.

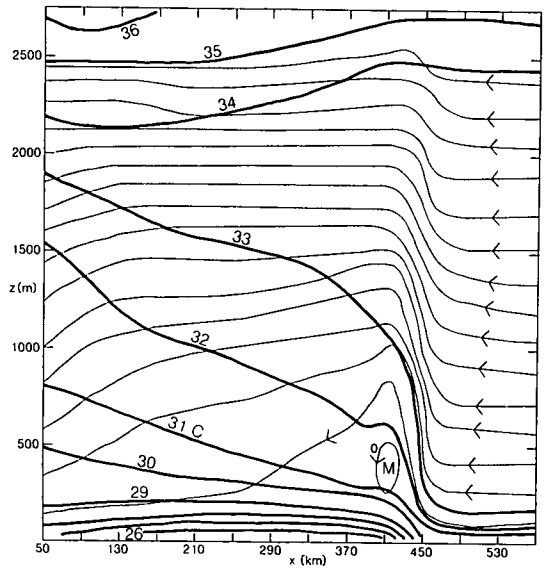

everywhere else the isentropic field is being distorted. It is suspected that, in the real atmosphere, even in the absence of a sea-breeze-conditioned presurge stable layer, this long wave gives rise eventually to finite amplitude wave trains in the nocturnal boundary layer. This appears to be the explanation of such wave trains arriving from the direction of the Gulf at the microbarometer array at Warramunga (Christie et al. 1979), 525 km inland. The sea-breeze system over land will of course be rapidly destroyed by stirring, due to begin with sunrise.

There has been no penetration limit imposed by Coriolis turning (Pearson 1973); it is evidently imposed by the length of the night, and a sea-breeze penetration of over 600 km is attained.

Results with geostrophic wind offshore (u_g negative)

This case differs in several ways from the u_g positive case, one of them being that the sea-breeze can now be definitively identified by a change in the sign of u.

The only 'single coast' experiments for this case were performed with $u_g = -5$ m s^{-1}. Figure 4(a) shows isentropes and relative streamlines at an early stage, and (b) at a later one. The heating over land is evidently, as in the $u_g > 0$ case, tending to create vertical leading isentropes, while the motion is tending to tilt them backwards, rather than forwards, as in Fig. 1(a). The sea-breeze is an unsteady gravity current, the body of fluid within the $\psi = 0$ streamline moving with the front. The same can be said of the sea-breeze at a later stage, as shown in Fig. 5 for 2330 hr, but the volume of fluid moving with the sea-breeze front is now much shrunken.

Fig. 4 (a) As for Fig. 1, but ψ is now at intervals of 2000 kg m^{-1} s^{-1}; time 1320 hr; $u_g = -5$ m s^{-1}; $c_s = 0.6$ m s^{-1}; $w_{max} = 0.19$ m s^{-1} at 1130 m.
(b) As for (a). Time 1735 hr; $u_g = -5$ m s^{-1}; $c_s = 2.6$ m s^{-1}; $w_{max} = 0.28$ m s^{-1} at 1310 m.

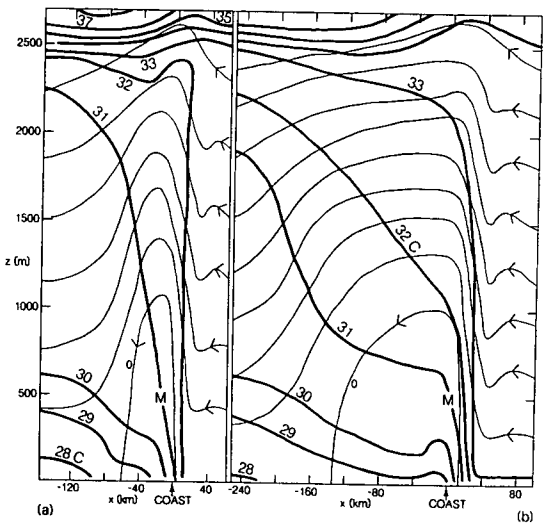

Fig. 5 As for Fig. 4(a). Time 2330 hr; $u_g = -5$ m s^{-1}; $c_s = 2.8$ m s^{-1}; $w_{max} = 0.07$ m s^{-1} at 680 m. M marks the position of the streamfunction minimum.

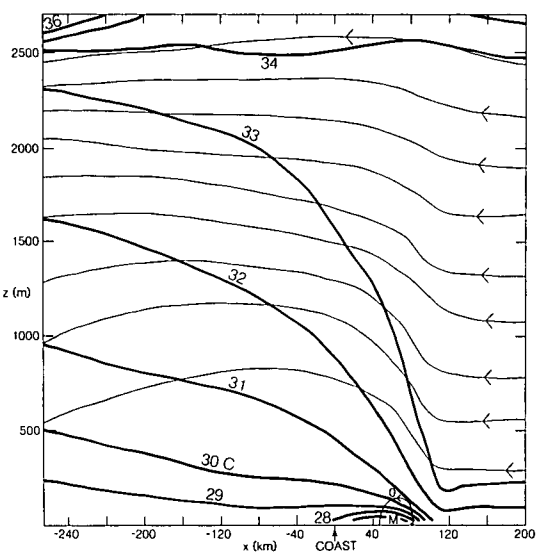

The wind components u and v during the development and decay of the sea-breeze are shown in Fig. 6(a) to (e). The sea-breeze, contained within the isopleth u = 0, reaches a height of about 800 m, and extends inland, but much further seaward (about 270

Fig. 6 **Isopleths of u(x,z) and v(x,z) for $u_g = -5$ m s^{-1}.**
(a) Time 1430 hr; $c_s = 1.3$ m s^{-1}; $w_{max} = 0.25$ m s^{-1} at 1300m.
(b) Time 1810 hr; $c_s = 2.8$ m s^{-1}; $w_{max} = 0.25$ m s^{-1} at 1300m.
(c) Time 2130 hr; $c_s = 3.0$ m s^{-1}; $w_{max} = 0.12$ m s^{-1} at 820 m.
(d) Time 0100hr; $c_s = 2.0$ m s^{-1}; $w_{max} = 0.05$ m s^{-1} at 680 m.
(e) Time 0430 hr;$c_s = 1.0$ m s^{-1}; $w_{max} = 0.04$ m s^{-1} at 570 m.
M locates the maximum in v, which is represented by the thin line, while u is shown by the full line.

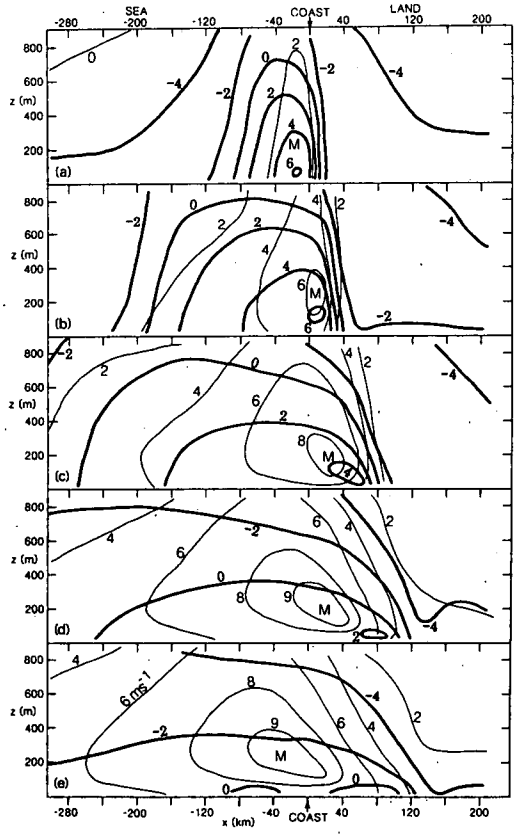

km at 2130 hr). The strong 'return flow' above the sea-breeze, occasionally exceeding 10 m s^{-1}, is not shown. By 0430 hr there is little of the sea-breeze left, and what there is, is split for a strip about 50 km wide about the coast by a weak land-breeze near the surface of less than 1 m s^{-1}. By 0500 the seaward branch of the weak onshore sea-breeze has vanished, and by 0600 hr the landward branch almost so. On the other hand, the action of the Coriolis turning has produced a coast-parallel jet, centred at 200 to 300 m above the surface, and extending progressively seaward.

The effects at the surface of the passage of a simulated sea-breeze surge

Numerical models, especially those as coarse as the 10 km grid used for the results reported above, do not succeed in simulating the sharpness of observed discontinuities. Changes at a given point over an hour starting at time t are shown in Table 1. In this table, the variables u, v, (wind components), T (temperature), R (mixing ratio), refer to the lowest model level (40 m), while p_o refers to surface pressure.

The only observations suitable for comparison with these modelled sea-breezes (at low latitudes) are surface wind records across the Peninsula (see Figs 21, 22 in CSR), which have been used to construct Fig. 10 in I and Fig. 1 in II. Once a sea-breeze has been transformed into a bore, it may be identified by its pressure signature, as well as, or better than by its surface wind response. At Highbury Station, near the middle of the Peninsula, the sea-breeze usually occurs about 2100 hr, and frequently shows a rather rapid pressure rise of about 0.5 mb or more. Sea-breeze surges occurring earlier in the day, especially before sunset, cannot readily be identified by their pressure signatures, nor can they at any time when the geostrophic wind is markedly offshore (i.e. on the western side of the Peninsula). The wind changes which mark the arrival of the sea-breeze surge is quite distinctive, consisting of a change from very variable speed and direction to a regime of much greater constancy, accompanied by a freshening and backing from a southeasterly to a northeasterly. The backing and freshening (Table 1) are well simulated by the model, as are the pressure effects in a more general way.

Horizontal extent of sea-breeze effects

Figure 7 summarises the results of the single coast experiments for four values of u_g at latitude $\theta = 16.7$°S in October, and two other combinations. Penetrations differ so little between grid spacings of 5 and 10 km that they could not be differentiated in this figure. Until about 1100 hr there is little genuine sea-breeze effect, the points on the graph representing rather the vertical velocity due to varying roughness between land and sea.

With $u_g = 12.5$ m s^{-1} the propagation rate c_s of the sea-breeze frontal surge remains less than u_g; with $u_g = 8$ m s^{-1}, c_s exceeds u_g after about 1800 hr; with $u_g = 5$ m s^{-1}, c_s exceeds u_g after about 1500 hr; with no geostrophic wind, c_s reaches a value of 7.0 m s^{-1} for both latitudes 35 and 16.7 at about 1900 hr, and maintains this value for several hours. At $\phi = 35$°S, maximum penetration is about 240 km, while for $\phi = 16.7$ it is about 360 km. For $u_g = -5$ m s^{-1} the sea-breeze penetrates about 120 km and reaches a maximum c_s of 3. 5 m s^{-1} about 1900 hr, having formed offshore, and come ashore about midday. It is just traceable at daybreak the next day. The evidence from the 'double coast' experiments described below is that with $u_g = -8$ m

Table 1. Changes in near-surface values of the variables with the passage of a modelled sea-breeze front, at a point x km from the coast.

u_g (m s^{-1})	t (hr, min)	x (km)	Δu (m s^{-1})	Δv (m s^{-1})	ΔT (°C)	ΔR (g/kg)	Δp_o (mb)
12.0	1900	355	1.3	0.3	−1.4	−0.3	0.27
8.0	1600	195	2.4	0.9	−0.7	− *	0.41
	2015	305	4.6	2.2	−3.2	− *	0.51
	2330	455	3.8	3.3	−3.7	− *	0.66
5.0	1110	45	1.9	0.2	0.3	−0.1	−0.02
	1600	135	3.5	0.9	0	−0.2	0.09
	2000	235	5.2	2.2	−3.5	0.7	0.57
	2400	395	5.0	2.8	− *	− *	0.58
	0500	605	3.7	2.3	−3.6	− *	0.47
0	1600	65	3.4	0.7	0	−0.5	0.03
	2015	125	5.2	1.6	−3.6	−0.3	0.40
	2300	205	5.6	2.7	−5.1	−0.6	0.51
−5.0	1600	15	1.2	0.9	−0.9	0.2	0.03
	2015	65	1.9	2.0	−2.7	1.0	0.14
	2400	95	0.2	0.9	−1.1	0.3	0.07
	0215	115	0.2	0.5	−0.7	0	0.01

* Computed but unavailable

s^{-1}, the sea-breeze does come ashore, is present with a near-surface wind of 1 m s^{-1} between 1800 and 2000 hr at a point 5 km inland, and recedes seaward about 2100 hr. When $u_g = -9$ m s^{-1} the sea-breeze does not come ashore, but remains as a shallow flow for the latter part of the day until 2130 hr, between 15 and 160 km offshore. For $u_g = -12$ m s^{-1} the sea-breeze out to sea reaches a maximum value of only 0.5 m s^{-1} 60 km out to sea, reaches seaward to over 100 km at about 1700 hr, and vanishes at about 1800 hr; while for $u_g = -13$ m s^{-1}, there is no sea-breeze anywhere, i.e. no reversal of u, although the surface wind component normal to the coast almost vanishes.

The seaward extension of sea-breeze effects with offshore geostrophic wind (and no component parallel to the coast) is surprisingly large, as shown in Fig. 6, and in the curve for x_r (Fig. 7). The lee coast effect actually spreads, according to the model, much further than is shown by x_r, in the form of a reduction in offshore wind component, and an enhanced low-level component in a coast-parallel direction (in the southern hemisphere turned clockwise from the geostrophic wind). The seaward extension of the sea-breeze is, unlike the landward, smooth and gradual, without sharp discontinuities. A low-level jet at 200 to 300 m, parallel to the coast, spreads seaward some 7 hours later than the onshore sea-breeze as shown by the graph for x_6 in Fig. 7.

The 'double coast' sea-breeze model

This is similar to the 'single coast' model, except that there are now two parallel coasts separated by a strip of land, and an extensive sea on either side. The uniform geostrophic wind, now necessarily positive, is onshore with respect to one coast (the 'windward' coast), and offshore with respect to the other (the 'leeward' coast). The width of the strip of land ('peninsula') was taken to be 440 km (the width of Cape York in the vicinity of Macaroni Station) in all but one experiment. In this the width was reduced to be similar (250 km) to that at Edward River, where bores are known to occur regularly (Neal et al. 1977; CSR).

Since the net solar short wave radiation (S_R) is what is ultimately responsible for sea-breezes and any bores resulting from them, one should be aware of the effect of a reduction in S_R, caused for example by cloud, on sea-breeze formation and progression. To serve this purpose, two experiments were run (with $u_g = 5$ m s^{-1}), with S_R arbitrarily reduced by (a) one-third, and (b) two-thirds of its computed clear sky value.

Horizontal resolution was varied: grid spacings of 10, 5, 3, and 1.5 km were used, with $u_g = 5$ m s^{-1}, in an endeavour to simulate as nearly as possible the events surrounding the transformation of sea-breezes into bores. All other experiments were performed with a 10 km grid.

A 'hill' experiment was designed; instead of the land being flat, as in all others, a hill of height 350 m, with its peak 100 km inland from the windward coast, curved smoothly to zero height at both coasts.

A 'baroclinic' experiment was also run. In this, a temperature gradient of 5 °C in 880 km (temperature increasing down the geostrophic wind of 5 m s^{-1} in the layer below the capping inversion) was imposed on the initial conditions, with geostrophic ('thermal wind') balance in the initial fields of v_g.

In general, v_g, the coast-parallel component of geostrophic wind, was set to 0, since earlier experiments (reported in I) showed that this had little ef-

Fig. 7 **Inland penetration, x_s, determined by maximum vertical velocity, of modelled sea-breeze surge fronts, plotted against time of day, for a variety of coast-normal geostrophic winds, and no component parallel to the coast. Except for the traces u_g = 12.5 m s^{-1}, and latitude ϕ = 35°S, the latitude is 16.7°S, z_0 = 0.02 m, and date is 1 October. For u_g = 12.5 m s^{-1}, ϕ = 16.0°S, z_0 = 0.16 m, and the date is 1 July; for ϕ = 35°S the date is 1 January.**

Also shown are x_r, the distance out to sea to which the reversal of u as a result of sea-breeze activity extends, and x_6, the seaward distance to which the v = 6 m s^{-1} isotach extends (see Fig. 6). x_r and x_6 are both negative by definition.

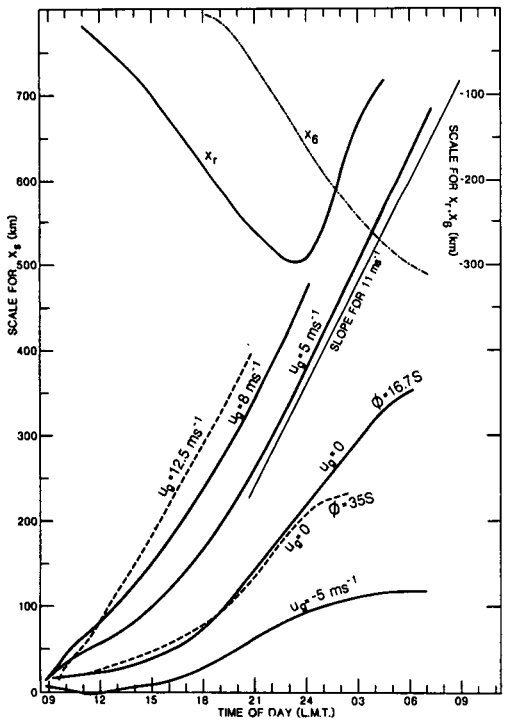

fect on sea-breeze penetration. However, for one experiment only, the values $u_g = v_g$ = 5 m s^{-1} were adopted, to explore the effect of v_g on bore formation.

To test whether the depth of convection over land might be an important factor in bore formation, an experiment was run in which the initial temperature and humidity were those measured at Macaroni Station on 10 October 1981, instead of those on 6 October (see Fig. 11 of II). In the former, the capping inversion was at 4000 m instead of 2700 m.

To investigate the effect of varying u_g on bore formation, 12 experiments with values of u_g spanning the range 1 to 15 m s^{-1} have been carried out, covering most of the observed range of u_g on Cape York in October. Since the two sea-breezes do not interact with each other during the daytime, this gives an opportunity to test the applicability to sea-breezes of the laboratory experimental results of Simpson and Britter (1980), concerning the effect of a pre-existing velocity U_2 on the speed of a gravity current. Their results showed that, if the 'effective gravity' (g′) and height (h) of a gravity current are kept constant, the speed of the gravity current is increased by α U_2. Figure 8 supports approximately the value 0.62 for α found by these authors when the geostrophic wind assists the sea-breeze; when the geostrophic wind opposes it, the value of α is much smaller. The values of all controlling parameters are kept constant, except for u_g, in the numerical experiments, and g′ and h are allowed to find their own levels.

Bore formation: the clashing of sea-breezes

The results show that, as expected from the single coast experiments, sea-breezes form on both sides of the peninsula, one assisted, the other resisted, by the geostrophic wind. Eventually (after nightfall) the former became more vigorous, in terms of energy and depth, than the latter. Provided the uniform and constant geostrophic wind is of a suitable magnitude, both absolutely and relative to the width of the peninsula, the two sea-breezes must collide, nearer (for $u_g \neq 0$) one side of the peninsula than the other.

Figure 9 is the double coast equivalent of Fig. 7. The results for u_g >12 m s^{-1} (i.e. 13 and 15 m s^{-1}) are not shown, since these integrations produce no new features; nor are those for $u_g = v_g$ = 5 m s^{-1}, which are closely similar to those for u_g = 6, v_g = 0 m s^{-1}. An upper limit to u_g for which bores

Fig. 8 **The value of $\alpha = \{\bar{c}_s(u_g) - \bar{c}_s(0)\}/u_g$ as a function of u_g, where u_g is the coast-normal geostrophic wind, and v_g = 0. $\bar{c}_s(u_g)$ is the mean speed of a sea-breeze surge between 1200 and 1800 hr at latitude 16.7°S in October. The change in the value of α in the vicinity of u_g = 0 is not due to Coriolis effects, as demonstrated by an experiment with f = Coriolis acceleration = 0, which showed virtually no change. The thin line marks the value of α found by Simpson and Britter (1980) for laboratory gravity currents, in which u_g was replaced by U_2, the ambient flow.**

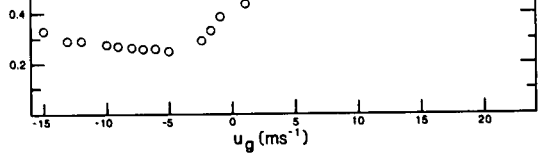

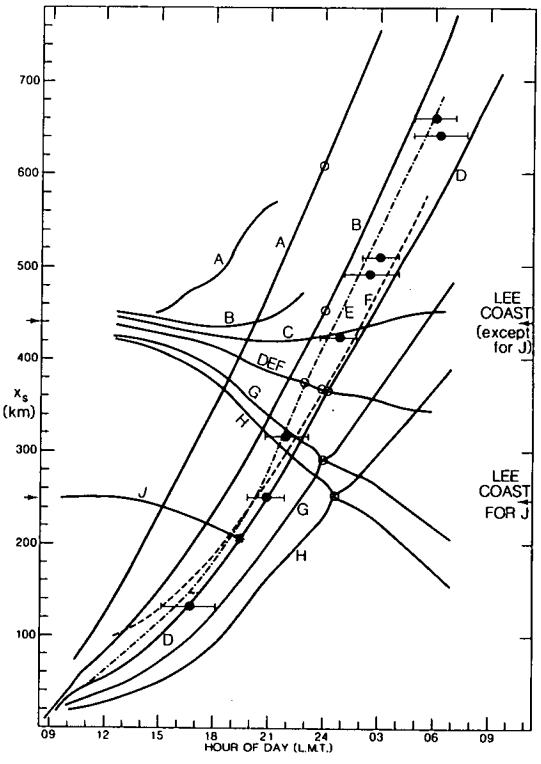

Fig. 9 **Distance of modelled surges (sea-breeze or bore) from the windward coast for the 'double coast' experiments. The surges (located by w_{max}) are in each case sea-breeze fronts (referred to as 'major' from the windward coast, and 'minor' from the leeward) until the time of collision, marked by a circle; thereafter they are bores rather than gravity currents. Mean (and twice the standard deviation) arrival times of observed discontinuities at several places located in Figs 9 and 10 of I are also shown.**

A: u_g = 12 m s^{-1}, flat land, initially horizontally uniform temperature and humidity.

B: as for A, but u_g = 8 m s^{-1}.

C: as for A, but u_g = 7 m s^{-1}. Only the minor surge is shown, the major, closely following E, being omitted for clarity.

D: as for A, but u_g = 5 m s^{-1}.

E: as for D, but with initial temperature below the capping inversion increasing by 5 °C over the 880 km of the horizontal domain (i.e. from x = −220 to x = 660 k).

F: as for D, but with a hill near the windward coast, as described in the text.

G: as for D, but with u_g = 2.5 m s^{-1}.

H: as for D, but with u_g = 1 m s^{-1}.

J: as for D, but with the width of the 'peninsula' reduced to 250 km. The major surge is omitted to avoid congestion, since it follows D closely, lagging it very slightly after the collision, marked by an asterisk, at about 1945 hr.

Note that there is no bore moving upstream (against the geostrophic wind) for u_g greater than about 6 m s^{-1}, but that for smaller u_g the surge from the leeward coast continues to propagate as a bore at about the same speed, after collision.

may form somewhere (under the conditions of the experiments) is evidently greater than 15 m s^{-1}, but for values of u_g greater than about 8 m s^{-1} the bore is increasingly diffuse and far downstream, as shown in Fig. 10. In this figure the values of x_s and w_{max} at the time when bore formation begins (i.e. the time of appearance of the hump of cool air in the isentropic field) are plotted against u_g. The value of w_{max} in this figure is taken to be an index of bore intensity. It is noteworthy that with $u_g > 8$ m s^{-1} transformation of the wind-assisted sea-breeze front to a bore is not instantaneous. It requires 2 to 3 hours after the beginning of bore formation before the disturbance is moving as a pure wave, with no closed circulation, rather than as a partial gravity current with excess velocity at some level just behind it.

Under the conditions investigated, bore formation occurs over the peninsula if $u_g < 7.5$ m s^{-1}, and off the lee coast for greater u_g. For a peninsula of width 440 km there is no lower limit on the magnitude of u_g for bore formation, and if u_g is small enough ($\leqslant 7$ m s^{-1}) not one, but two bores are formed, moving with speeds similar to those of the sea-breeze surges which evidently energised them.

Although the results of the collision are by no means independent of horizontal resolution in the model, especially in regard to the sharpness of the bore and its following undulation, there is a surprising unanimity (with u_g = 5 m s^{-1}) with regard to propagation speed of both bores and sea-breezes. Hence all other experiments have used a horizontal resolution of 10 km.

Figure 11, from the 1.5 km grid, with u_g = 5 m s^{-1}, displays the surface pressure deviation δp_o from its initial value, plotted against x for a succession of times, from just before the collision of the sea-breeze fronts to about 2 hours after. The sequence of events is clear: the stronger, deeper sea-breeze surge, moving in the positive x direction at about 10 m s^{-1}, impinges on the weaker, moving in the opposite direction at about 1 m s^{-1}, and forces the cool surface air rapidly upward, forming a sharp hump of cool air and a pressure peak moving at approximately the speed of the stronger gravity current. This process apparently continues (in this case for about 10 minutes) until some critical condition is met; when this point is reached, bore formation is triggered. In this case, the hump remains station-

Fig. 10 **The distance x_{sb}, of the sea-breeze surge from the windward coast at the time of bore formation, as indicated by the first appearance of a bulge in the isentropes (read out at half-hourly intervals). The value of w_{max} at this time is also plotted. The locations of the lee coast and the furthest station in the observing network, MM, are shown.**

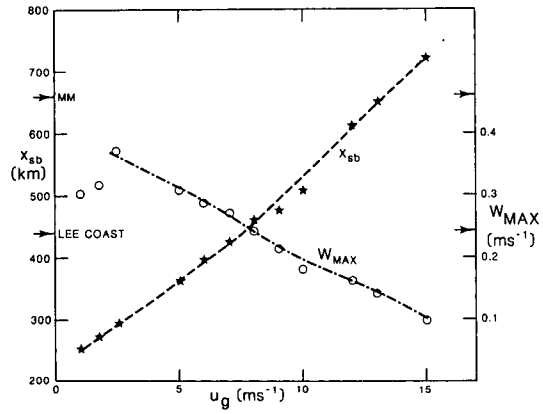

Fig. 11 **Showing the time sequence (hours and minutes) of modelled surface pressure distribution before, during, and after the collision of two sea-breeze surges. δp_o is the deviation from its initial value. These results relate to the 1.5 km experiment. The maximum vertical velocity (always found in the height range 1000-1400 m) at a succession of grid-points passed by the disturbance is shown at the top.**

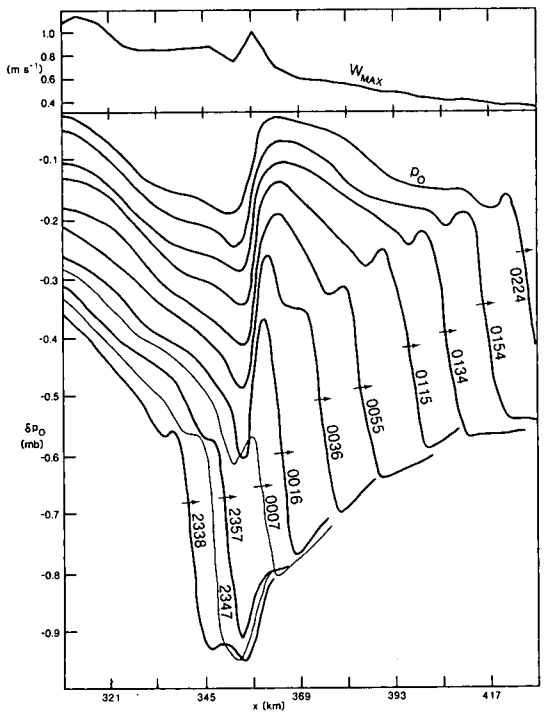

ary, while the bore moves out from it, at roughly the speed of the 'major' gravity current before impact.

If we look at the sequence of vertical velocity at, for example, 500 m, as in Fig. 12, we see that the two maxima approach one another, merge, and then split again, one branch remaining stationary at x = 357 km, the other moving off with the bore. The strong wind component, u, located behind the erstwhile major sea-breeze surge, remains stationary after impact, and is responsible for the stationary maximum in vertical velocity. Behind the bore, on the other hand, u is everywhere less than the speed of the bore, c_b.

The bore rapidly becomes undular, but with only one wave crest; later a very weak second crest appears in the lower-level streamlines, and by 0500 hr three crests of very small amplitude are discernible at a height of about 1000 m. The 'half-wavelength' from leading crest to trough varies between two and three gridlengths, i.e. 3 to 4.5 km, but the amplitude is puny, about 0.02 mb, and variable. Vertical displacement of the streamlines in the half-wavelength is at most little more than 100 m, less that 1/5 of the magnitude of observed values (see Fig. 5(a) to (c) in II and Fig. 13 in CSR).

Fig. 12 **Vertical velocity, w, at z = 500 m, as a function of x, from a time just before to some time after the collision of the two sea-breeze fronts (1.5 km grid). Horizontal line segments mark w = 0.**

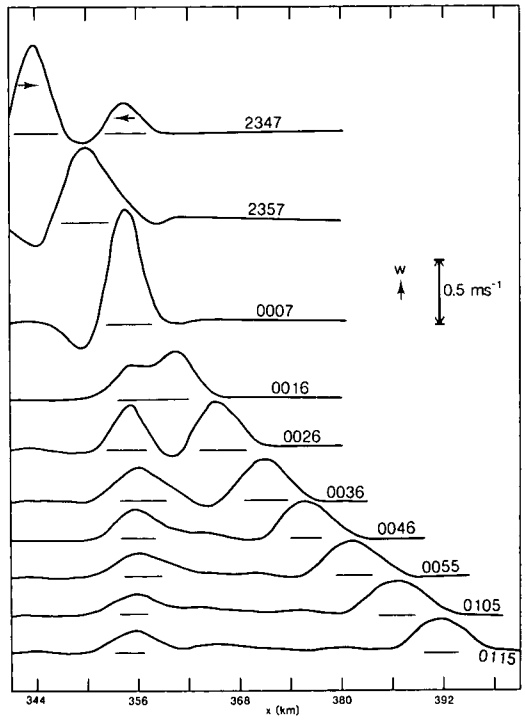

When the asymmetry between the sea-breeze surges is smaller, as in the case of u_g = 1 m s^{-1}, Fig. 13 shows that the initial hump gives rise, as one would expect, to two bores, moving in opposite directions, with speeds similar to those of the erstwhile sea-breezes.

The processes of bore creation and maintenance are illustrated by the relative streamlines and isentropes of Figs 14 and 15, relating respectively to an early and later stage of bore formation. In both cases the close parallelism of isentropes and steamlines about the leading edge indicate steadiness (in a frame moving with the bore) in this part, which is moving towards the leeward coast at a speed of about 10 m s^{-1}, while the cold air behind the leading edge is being carried upward to form the plateau of cold air and high pressure to the rear of the leading edge. At the later time (Fig. 15) the bore is more nearly steady, while in Fig. 16 we show a still more steady-state bore, from the 3 km resolution computation.

It is worth noting that the vertical motion about the bore's leading edge is damped rapidly with height above the capping inversion at about 2700 m.

Integrations with the coarser grids (10, 5, 3 km) produce similar results to the finest (1.5 km). In each case there is a sudden lifting of the cool sea-breeze air and the formation of a bore. The differences relate to details such as the horizontal scale of the disturbance. For each of the four resolutions the bore is undeniably present, and its properties apparently as similar as the resolution differences will allow.

Fig. 13 **Similar to Fig. 11 for 10 km grid and u_g = 1 m s^{-1}. The outward spread of a bore from each side of the hump of cold air raised by the collision is demonstrated. Parts of the pressure field in the inner region are omitted for clarity.**

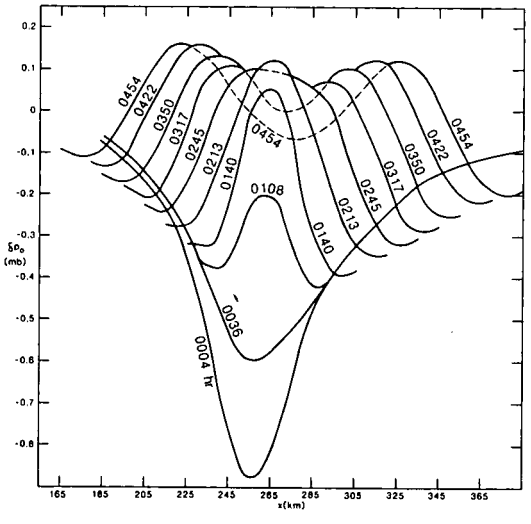

Fig. 14 **Isentropes and relative streamlines at a time just after bore formation, viz 2356 hr. The speed of the bore, c_b, is 9.2 m s^{-1}. Streamline channels represent 1000 kg m^{-1}s^{-1}. M marks a streamline minimum (1.5 km grid).**

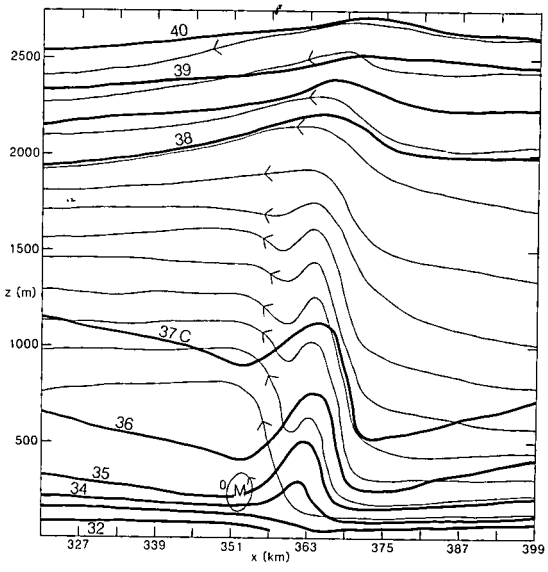

Fig. 15 **As for Fig. 14, but 1.5 hr later (0126 hr). c_b = 8.8 m s^{-1}. The bore is still over land, near the leeward coast.**

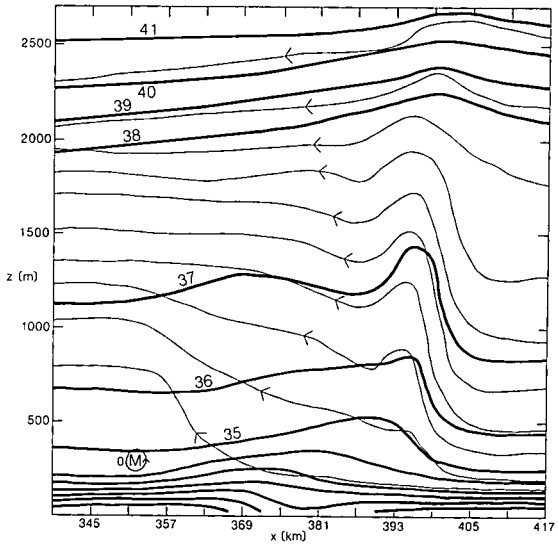

The 'origin' of the air behind the bore

It is of the nature of bores that they move more rapidly than the fluid behind them. That this is so in the case of the simulated bore of Fig. 16 is shown by the wind field in (a). The bore is moving at least 4 m s^{-1} faster than the wind behind it.

Fig. 16 **Wind and potential temperature in an atmospheric bore. Time is 0300 hr; u_g = 5 m s^{-1}. The bore is now 20 km off the lee coast, and moving at 10.7 m s^{-1} (3 km grid).**
(a) The two components of wind, u (full lines) and v (thin). M marks the maximum in v.
(b) Isentropes (full lines) and relative streamlines (thin) up to 4000 m, at intervals of 2000 kg m^{-1} s^{-1}.

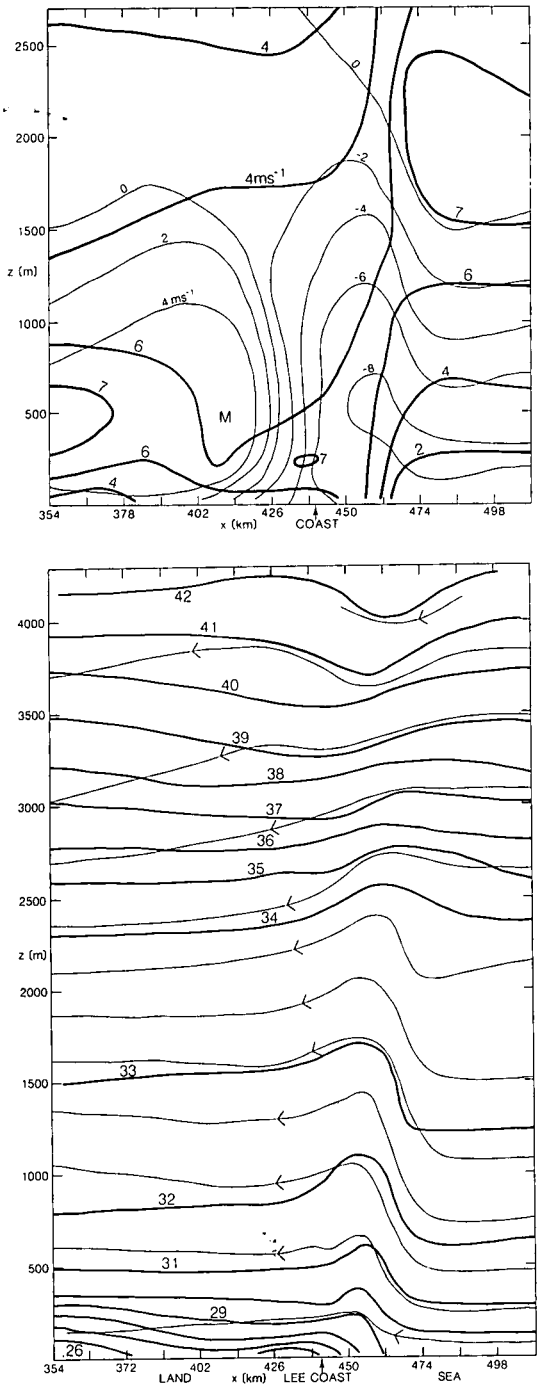

It had been deduced from radiosonde observations of Gulf bores that the air at a given point behind the bore some hours later must have recently been over the Coral Sea to the east of the Peninsula. To examine this question, a double coast trajectory experiment, with u_g = 5 m s^{-1} and grid spacing of 5 km was designed, in order to trace 30 air parcels through the windward coast sea-breeze and into the region behind the bore. It turned out that a parcel of air located, at 0530 hr, 160 km off the windward coast at 950 mb had moved by 2300 hr to be at 988 mb and 16 km behind the sea-breeze front (at x = 316 km), and by 0530 the next day to be located at 985 mb, 25 km off the leeward coast, having travelled 625 km at a mean speed of 7.2 m s^{-1}. At that stage it was 75 km behind the bore. A further test was provided by tracing 30 parcels in the rectangle depicted in Fig. 17(a), behind the principal sea-breeze surge at 2300 hr over the next 6.5 hours. They were then found to occupy a volume shown by the curved shape in Fig. 17(b). That portion of the original rectangle which, 6.5 hr later, was within 87 km of the bore is shown inside the rectangle in Fig. 17(a). The parcel which at 2300 hr was subsequently nearest the bore is marked by an asterisk. At 0530 hr this parcel was falling behind the bore at about 3 m s^{-1}. There is nothing detectable in the temperature, humidity, wind or pressure fields to distinguish that part of the air which has been advected from the windward ocean from that which has been forced to ascend from near the surface.

Depth of the bore

The model results show clearly that the bore is mainly confined to the layers comprising the daytime mixed layer (Fig. 16). The capping inversion partakes only slightly in the vertical motion, which is damped strongly with height above the 'fossil' mixed layer. Any cloud below the capping inversion may be slightly enhanced with the passage of the bore, and this has been observed in time-lapse movies.

Effects of the bore on near-surface variables

Changes in the near-surface variables one hour after the time t of the passage of the bore are shown in Table 2, for which only the 10 km grid results have been used.

Figure 16 in CSR and Fig. 3 in II show that, with pronounced morning glories, the initial pressure jump is usually about 1 mb over about 5 minutes, at places on the western side of the Peninsula, at Mornington Island and at Burketown. The model results suggest that there should be a strong negative correlation between the magnitude of the pressure jump and u_g, whereas the observations in III show only a weak but significant correlation at Normanton and none at Mornington Island. The reason for this failure in the model cannot be stated with certainty, but may be due to resolution deficiency and even more to the three-dimensional nature of

Table 2. Changes over one hour in near-surface variables with the passage of a modelled bore, at a point x km from the windward cost.

Special feature	u_g (m s^{-1})	t (hr, min)	x (km)	surface	Δu (m s^{-1})	Δv (m s^{-1})	ΔT (°C)	ΔR (g/kg)	Δp_o (mb)
	15	0110	785	sea	3.0	4.4	−0.1	1.0	0.18
	15	0215	865	sea	2.8	−*	0.2	−*	0.07
	12	0215	725	sea	3.7	6.2	−0.3	0.7	0.20
	10	0215	625	sea	3.2	7.2	−0.2	−0.6	0.17
	8	0210	555	sea	5.5	2.2	−0.3	1.7	0.55
	5	0105	405	land	5.9	1.6	−0.4	−0.5	0.55
	5	0210	435	land	4.9	2.3	−1.3	−1.3	0.43
S_R reduced	5	0420	465	sea	3.4	1.8	−0.6	−*	0.17
by a third	5	0525	495	sea	3.9	2.6	−0.2	−*	0.19
v_g = 5 m s^{-1}	5	0210	455	sea	6.6	4.7	−0.7	−1.9	0.43
hill	5	0105	405	land	3.8	2.8	−0.7	−0.7	0.46
hill	5	0230	460	sea	3.5	1.3	−0.4	−0.3	0.29
baroclinic	5	0005	425	land	8.2	6.4	−1.1	−*	1.00
baroclinic	5	0250	545	sea	9.2	6.8	−1.1	−*	0.61
high	5	0105	405	land	5.6	1.6	−0.4	−0.4	0.62
inver-	5	0210	435	land	4.3	1.7	−1.1	−1.1	0.46
sion	5	0340	505	sea	3.9	0.8	−0.3	1.0	0.33

* Modelled but unavailable

Fig. 17 (a) Isentropes at 2300 hr, about an hour before the collision of the sea-breezes, which are moving at 9.6 and −1.6 m s^{-1} respectively. The rectangle encloses the air parcels whose subsequent history is traced, as in the text. The stippled area encloses those later found to be nearest the bore, as shown in (b).

(b) Relative streamlines at 0530 hr. The bore is moving at 10.2 m s^{-1}. The curved figure encloses the parcels shown in the rectangle in (a). The stippled area encloses those in the stippled area of (a), 6.5 hr earlier. The asterisk marks the location of the parcel now nearest the bore (5 km grid).

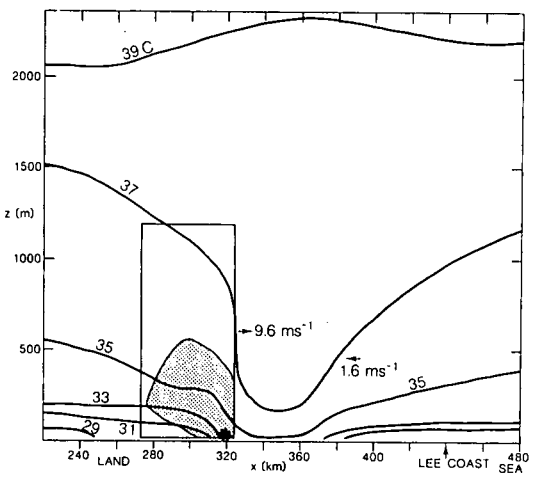

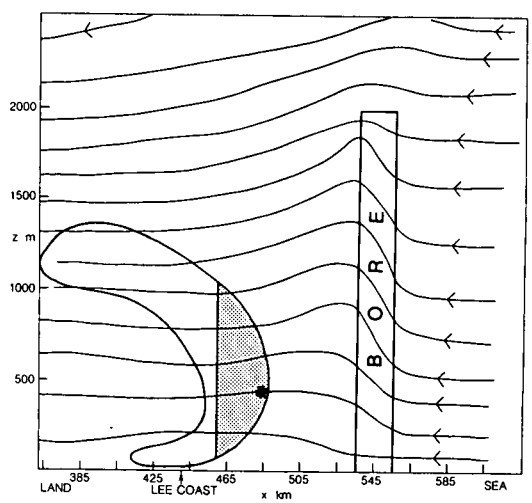

the Peninsula-Gulf events. The most important aspect of Table 2 is that the modelled pressure jumps are only about half as strong as the observed ones, and that the magnitude of the jump can be markedly increased by assuming initial baroclinicity, and considerably less so by having a deeper convective layer than was assumed in most of the modelling work.

Discussion

Horizontal extent of sea-breeze circulations: observational evidence

The surprisingly great inland and seaward penetrations achieved by sea-breeze circulations in low latitudes, with dry conditions and coast-normal geostrophic wind, is supported by observation.

1. During the Koorin Expedition in the winter of 1974 (Clarke and Brook (eds) 1979) obvious sea-breeze occurrences were recorded, in the evening of most of the 29 nights of operation, on one occasion with an onshore geostrophic wind from the Gulf of about 12.5 m s^{-1} (J. R. Garratt, personal communication). The site at Daly Waters was chosen to be representative of a fairly uniform terrain far enough removed from the coast (280 km away to the east-northeast) to be devoid of strong advective effects, as one would expect with a geostrophic wind from a direction south of east. The coast in that vicinity is also strongly curved in such a sense as to reduce sea-breeze penetration. In the event, the geostrophic wind was onshore with respect to the Gulf coast (and never from a direction south of east), with a component averaging 8.7 ± 3.4 m s^{-1} on every evening, so that sea-breezes at the formative or mature stage should have been expected on the basis of the current numerical experiments.
2. D. R. Christie (personal communication) affirms that 'sea-breeze influences' in the form of surface pressure wave trains, detected by his array of microbarometers at Warramunga, near Tennant Creek (525 km inland from the Gulf) are not infrequent, and arrive between 0200 and 0900 hr.
3. The author's observations across Cape York (see I and CSR) show quite clearly a progression of the east coast sea-breeze front for well over 300 km.
4. The Admiralty (1944) quotes results of the Snellius Expedition, led by P. M. Van Riel, in the eastern part of the Netherlands East Indies in 1929-30, who observed what were interpreted as sea-breeze influences on the surface wind '200 miles' downwind (at latitude 4 °N) from the land mass of Borneo. This 'influence' reached a maximum deviation of about 4 m s^{-1} at 2000 hr, and was still detectable at 0200 hr. This agrees at least qualitatively with our model results for surface wind off a lee coast (see Fig. 6).
5. A limited amount of information is available about low-level winds around the Gulf of Carpentaria before the onset of the bore. Focusing on the time of day just before the normal arrival time of the Gulf bores, we note the following (for locations see Fig. 9 of I).

At Karumba, the averages published by Neal et al. (1977) for 0130 hr on morning glory days show a low-level jet at about 300 m from south-southwest of 1 to 2 m s^{-1}.

At Macaroni Station, 22 km inland on the western side of the Peninsula, in 1981, upper wind observations at about 2300 hr usually showed a low-level jet, clearly the remnant of a sea-breeze. The mean of eight such observations was 7 m s^{-1} from the southwest at a height of 270 m.

At Birri Beach, 175 km off the lee coast of Cape York, inspection of the surface wind records for October 1981 showed that the direction of the wind before the arrival of the bore (as judged from the anemograph) at about 0530 hr was always from the south-southwest. The model predicts 6.2 m s^{-1} from 197 deg., if the geostrophic wind off the Peninsula coast is 5 m s^{-1}.

More variable are the pre-bore low-level winds at Burketown, about 140 km off the lee coast of Cape York, but also on the northern edge of a diurnally heated continent. Available information about the low-level winds prior to a Gulf bore at Burketown is given in Table 3.

Although there is apparently always a low-level wind maximum, it is not always from a similar direction to those observed at other places around the Gulf listed above. The model results suggest the following explanation, based on two-dimensional modelling.

Burketown's 0500 hr upper winds (up to about 500 m) may be tentatively hypothesised to be the result of sea-breeze activity the day before, either:

(a) at a point located 140 km off a straight lee coast (the east coast of the Gulf), oriented 025-205 deg. With $u_g = 5$ m s^{-1}, $v_g = 0$, the model yields a low-level jet of 8.6 m s^{-1} from 190 deg. at 300 m (0500 hr);

or

(b) at a point near a straight coast oriented 300-120 deg. (i.e. the south coast of the Gulf), with no geostrophic wind, in which case there should be a low-level jet from 320 deg. of 6.1 m s^{-1} at 200 m, according to the model.

Table 3. Height, direction, and speed of the low-level jet at Burketown before the arrival of a bore from the east-northeast.

Date	29/9/79	4/10/79	8/10/80	10/10/80	11/10/80	13/10/80	11/10/81	20/10/82
Height of jet(m)	100	112	358	252	257	228	257	200
Direction(deg)	190	254	203	283	304	241	188	233
Speed (m s^{-1})	2.0	3.9	7.6	7.6	8.2	4.7	8.0	~7

The eight days' observations available show that there is a jet on all such occasions, and suggest that it is one or the other or a combination of both hypothesised types of response. Thus the Burketown pre-bore wind at low levels tends to be dominated by fossil sea-breezes from the terrestrial heating of the day before.

The effect of reducing net solar radiation (with $u_g = 5$ m s^{-1})

As would be expected, a reduction in S_R has a considerable reducing effect on sea-breeze activity. A one-third reduction results in a weakened windward coast sea-breeze, with maximum vertical velocity 0.16 m s^{-1} at 2015 hr and inland penetration 270 km at 2300 hr, compared with values of 0.29 m s^{-1} and 320 km with full radiation. The lee coast sea-breeze penetrates only 3 km inland (at 2200 hr), compared with 70 km when S_R is unreduced. The two sea-breezes meet about 10 km off the lee coast, and produce a weak bore, as shown in Table 2.

When S_R is reduced to only 1/3 of its clear sky value, the wind-assisted sea-breeze is much further reduced in vigour: maximum vertical velocity reaches only 0.05 m s^{-1} and 2300 hr penetration only 200 km. The lee coast sea-breeze remains well offshore; the two sea-breezes do not meet; and no bore ensues.

The effect of orography

The effect of a coastal escarpment of height about 600 m on sea-breeze development has already been discussed in I (see p. 137). The finding there is probably equally valid on the eastern side of the Peninsula in October. The hill induces an anabatic circulation during mid-morning, which masks the sea-breeze; later in the day, a sea-breeze surge develops in much the same way as it would have in the absence of the escarpment.

A question to be answered is whether the orography of Cape York plays an important role in producing the morning glory. One might expect the long slope to the west to accelerate the sea-breeze surge once it had formed near the top of the hill, and that this could result in a stronger interaction of sea-breezes on the western side of the Peninsula. Figure 9 shows that the easterly sea-breeze surge in the 'hill' case does indeed remain ahead of a similar surge on flat land throughout its career, but the difference is not great, and the computed bore is certainly no stronger. Since, however, stronger smoothing had to be used for the hill model, the strength of the bores produced, as indicated in Table 2, are not strictly comparable. Nevertheless, it is safe to say that the east coast escarpment on the Peninsula, while it affects the easterly sea-breeze surge in its early stages, has little effect on the production of bores near its western side.

The speed of the bore

The sequence of events portrayed by the model for $u_g = 5$ m s^{-1} is credible: the stronger gravity current appears to lift the almost passive fluid in the weaker one (i.e. the pre-conditioned coastal strip of air deduced in II), although there is no striking difference in their densities, until the uplift is sufficient to form a bore. In a notional sense, this requires that condition 7 in II should be satisfied

$$c_o > c_s/F + u_i(1 - 1/F) \qquad \ldots 1$$

where c_o is the velocity of small amplitude waves in the invaded medium, c_s the velocity of the major sea-breeze surge, u_i the velocity of the air in the invaded medium, and F is a monotonically increasing function of $\delta h/h_i$, the normalised lifting of the air in the 'minor' sea-breeze. Once the bore is formed, it translates with a speed notionally described by simple bore theory

$$c_b = Fc_o - u_i(F-1) \qquad \ldots 2$$

If $\delta h/h_i$ and thus F in Eqn 1 is just sufficient to satisfy criterion 1, then, approximately

$$Fc_o = c_s + u_i(F-1)$$

whence, notionally,

$$c_b = c_s$$

and the bore velocity is equal to the erstwhile major sea-breeze surge velocity. This is, as nearly as can be observed, exactly the case.

The hump of cold air raised by the intruding sea-breeze front might be expected also to produce a bore propagating in the reverse direction, and the model supports this when u_g is small enough, i.e. when the sea-breeze surge from the leeward coast is fast enough. One may note in passing that the production of bores by supercritical katabatic flow over a discontinuity in slope also produces two bores, one propagating upstream, the other downstream (Clarke 1972). Although both the katabatic model and the colliding sea-breeze model (with sufficiently small u_g) both produce two bores, the upstream propagating member has not, so far as is known, hitherto been observed in nature.

Figure 12 shows that, at the point of bore creation, a residual ascending motion, a standing wave or hydraulic jump, persists, while the bore moves off. This implies that the short-lived cataclysm of the clash of the surges may produce a cloud bank, out of which the bore cloud emerges. It is believed that two such events have been witnessed, one near Dunbar Station, about 2300 hr on 2 October 1979, and the other about midnight near Macaroni Station, 13-14 October 1981. In the first, the clash apparently produced a sharp shower to the east of the observer (the only rain on the Peninsula network that night), but the cloud gradually dissipated, while a thin roll detached itself, came over the observer, and finally also dissipated. The pressure trace of the first of these events is included in Fig. 16 of CSR, and of the second in Fig. 3 of II.

The speed of the bore is governed, in the case of a steady state bore, by its amplitude and the static stability and vertical wind structure in the medium

through which it is propagating, as set out notionally in the simple bore equation (Eqn 2). This must be regarded as providing nothing but an analogue between the relatively simple situation of a liquid flowing in a channel and a naturally occurring internal bore. Accepting this analogue for the time being, we can inquire what the numerical model has to say about the heights at which u_l and δh should be measured for the simple bore equation (see II, Eqns 1 and 2)

$$c_b = u_l + F(c_o - u_l)$$

where $F = \{1 + 3/2\ \delta h/h_l + \tfrac{1}{2}(\delta h/h_l)^2\}^{\frac{1}{2}}$

to yield a correct value for the bore propagation speed c_b.

It turns out that the bores produced by the model propagate through a medium in which the term involving u″ (see Eqn 6 in II) is quite negligible compared with the term in N^2, which occurs in Eqn 5 of II. If we use this equation to estimate c_o, and the model output to determine $u_l(z)$ and $\delta h(z)$, and assume h_l to be the depth (about 1000 m) of the near surface stable layer, we find, from the 1.5 and 3 km grid model results, that if the wind component u_l and the lifting δh (defined by the increase in height of a streamline at the bore) are given the values of a parcel initially at about 300 m, the value derived for c_b is near that observed. This finding agrees approximately with that in II that 'the middle layer of the oscillating inversion' in naturally occurring bores is the level to look for the values of the variables which give an approximately correct value for the propagation speed.

The reason for the term involving u″ being negligible in the model and not in the real case, is that the geometry of the latter, unlike that of the former, is three-dimensional. The real lee coast sea-breeze, instead of being (at night) nearly parallel to both the leeward and windward coasts, and therefore to the major sea-breeze surge, is parallel to the lee coast, but inclined at a considerable angle (about 38 deg. in the case of the Peninsula) to the windward coast and its sea-breeze surge .Thus, in the real case, $u_l<O$ and $u''>O$ has a positive value comparable with $-N^2/(u_l - c_o)$ in low levels.

Orientation of the bore

When the peninsula is narrowed to 250 km, the two sea-breezes collide earlier (about 1945 hr with $u_g = 5$ m s^{-1} as opposed to 2330 hr when the width is 440 km). Bore formation occurs as before, the bore propagating at almost the same speed. The diminution in x_s is less that 10 km in 450 by 0245 hr. The experiment shows that the progress of the bore is not strongly dependent on the width of the 'peninsula' within the limits studied. This explains why the orientation of a bore produced by a tapered peninsula, such as Cape York, is very nearly that of the windward coast, (if the geostrophic wind is nearly uniform along the Peninsula) in agreement with many observations.

The life history of the bore

Despite the diagrams showing relative flow through the bore from the front, Fig. 17 shows clearly that, some distance behind the bore, increasing with time, is found fluid which was originally behind the major sea-breeze front. Thus the bore may be said to embrace some of the properties of the originating gravity current. The process of loss of sea-breeze air behind the bore wave is strongly reminiscent of Maxworthy's (1980) account of the loss of dyed fluid behind his solitary wave.

Sea-breeze air can penetrate far inland without being turned aside by Coriolis acceleration, if its inland component of motion is geostrophic. Excess of such motion over geostrophic results in Coriolis turning, so that v increases (in present circumstances) and u regresses towards geostrophic. The ultimate effect of the bore will be to replace the fossil lee coast wind structure (due to heating over the land during the previous day) by a geostrophic forward velocity, and a lateral velocity opposite in sign to the pre-existing one. This is what is observed in the Gulf area, where a well-developed bore replaces a south-southwest wind by a northeasterly one. Model results show that strong u_g should result in weak bores forming well out to sea, with preceding southerly or southeasterly winds.

The supergeostrophic component u behind the bore in Fig. 17 up to about 1000 m must eventually decline to geostrophic, thus producing descent behind the bore, and eventual cutting off and degeneration to a train of solitary waves, such as have been investigated by Christie and Muirhead (1983). The model has not been used to pursue the fate of the bore to its end, because of obvious limitations. However, the further the modelled bore propagates, the nearer does it approach the state of being cut off. The results from the 10 km grid, which naturally cannot resolve the solitary waves described, e.g. by Christie et al. (1979), give the following, (Table 4) where h_o is the height of a streamline before the bore, h_b the height of it immediately after, h_{60} the height 60 km behind the bore, and h_{150} the height 150 km behind.

Table 4. The height, for two different times, of a streamline just before, just after, and some distances after the bore ($u_g = 5$ m s^{-1}).

time	h_o	h_b	h_{60}	h_{150}
hr, min	m	m	m	m
0330	672	1563	1333	-*
0603	617	1221	933	786

*bore absent.

It will be seen that in the first case (0330 hr), after 60 km the bore had decreased in depth by 26 per cent, while at 0630 hr it had decreased by 48 per cent. Af-

ter 150 km it had decreased by as much as 72 per cent.

Regarding the dual nature of the Gulf bores, it will be noted that the sudden changes are concentrated at the bore, which is in essence a sudden onset of vertical advection, while the air advected horizontally from the windward ocean lags far behind, and cannot be readily identified by its properties. A parallel with the 'cool changes' of southern Australia will be recognised. Here the 'cold front' is diffuse and often cannot be precisely located (Garratt et al. 1984), while the preceding 'changes' are frequently swift and dramatic.

Changes in the temperature profiles following the bore's passage.

Several 'before and after' temperature soundings are shown in Fig. 9 of II. They show that, after some hours, there is a temperature reduction amounting at some levels to as much as 4 °C, or even more, in the lowest 2 to 3 km of atmosphere; above this is a slight warming, and often a lowering of the capping inversion. After the 'massive morning glory' described by Smith and Morton (1984), the cooling was up to 6 °C at about 1000 m, and the lowering of the inversion more than 300 m.

It is admitted that no changes of this magnitude have been produced by the models. The greatest were achieved by the 'baroclinic' model, where the 4 °C cooling in the lower layers decreased to zero just below the capping inversion. Above was a warming of about 1 °C. Other versions of the model performed similarly, but the cooling was less. The warming at and above the capping inversion appears to be due to adiabatic descent in a kind of lee wave.

The distinction between bore and sea-breeze

It is not true to say that the sea-breeze penetrates from Cairns to Burketown (650 km), even though air parcels reaching Burketown some distance behind the bore will have done so. The nocturnal sea-breeze is strong in the tropics, and penetrates far inland, lifting the stratified layer near the surface, but it does so at the expense of the available potential energy built up by solar heating over the land. It is an essentially unsteady phenomenon, continuously collapsing and flattening, and gradually changing its character from a gravity current to a kind of unsteady wave, with or without a closed circulation near its leading edge. Christie's evidence of 'sea-breeze influence' at Tennant Creek suggests that, in a single coast sea-breeze situation, the sea-breeze surge eventually produces wave trains in the stratified boundary layer through which it is moving.

A bore, on the other hand, although it must decay due to dissipation and radiative loss, is ideally a steady state entity. As a wave, it could last, in principle, a very long time, so long as it had a suitable medium in which to propagate. Over land, the heating of the low-level stable layer during the early forenoon must result in a rapid disintegration of the wave guide, and hence of the bore propagating on it. Over sea, in the presence of a suitable atmospheric structure, it may persist much longer.

There are, however, phenomena lying between these two. One is to be found when, with strong (12 to 15 m s^{-1}) geostrophic wind, a rapidly moving sea-breeze disturbance encounters the remnants of a lee coast sea-breeze well out to sea, and is gradually transformed, over several hours, into some semblance of a steady-state bore, slowly losing its strong, closed large-scale (hundreds of km) relative circulation.

The difficulty of classifying unsteady disturbances simply as gravity currents or bores is illustrated by Fig. 18, where (a) is, historically, a modelled degenerate sea-breeze, but certainly a wave rather than a gravity current, and (b) an unsteady bore some hours after creation by colliding sea-breezes.

The prediction of Gulf of Carpentaria bores

Evidently u_g is an important determining factor, but cloudiness, over the Peninsula during the day, determines the energy input, and must be even more important. The effect of clouds on sea-breezes and resulting bores has been rather crudely investigated by reducing solar input. Another important factor is evaporation, which depends strongly on soil moisture and could radically affect the creation of available potential energy. However, in typical September-October conditions on the Peninsula, the principal factor in determining when, where and how strong a bore will occur must be the geostrophic wind. If it is large, sea-breezes will tend to be diffuse,

Fig. 18 (a) An essentially unsteady wave associated with a degenerate gravity current (single coast). Time 0540 hr, u_g = 5 m s^{-1}, c_s = 11.7 m s^{-1}, w_{max} = 0.10 m s^{-1} at 970 m.
(b) A bore propagating with little change. Time 0530 hr, u_g = 5 m s^{-1}, c_s = 9.0 m s^{-1}, w_{max} = 0.06 m s^{-1} at 1200 m (double coast). Full lines are isentropes; thin lines relative streamlines.

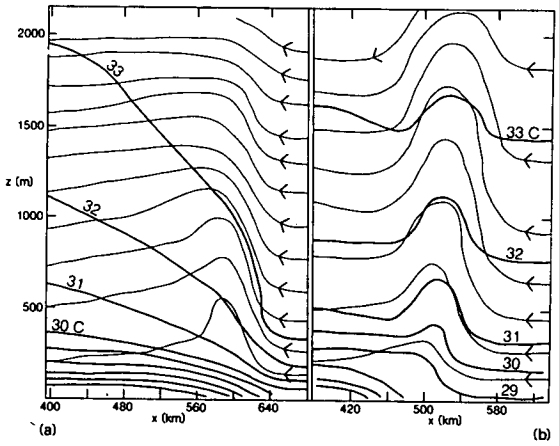

but the effect of the heating will ultimately be to produce a kind of interaction between the two bodies of cool maritime air when they meet, and this results in bore formation if the hump of cool air upthrust by the interaction is sufficiently pronounced. In the Gulf of Carpentaria, too strong a u_g (> 13 m s^{-1}) results in a bore forming too far west to be observed in the network (i.e. $x_{sb} > 660$ km), while, if it is too weak, the resulting bore may not reach the lee coast before it is destroyed by solar heating after daybreak. If one assumes that the time for this to happen is about 0900 LMT, our experiments show that (for $v_g = O$) the limits on u_g for bores to be observed in our network are about $1 \leqslant u_g \leqslant 13$ m s^{-1}, with stronger bores being favoured by weaker u_g and stronger baroclinicity. These conclusions are in reasonable agreement with the observations in III, except that no data exist on baroclinicity.

The lack of observed bores with $v_g < O$ (a rare condition, met on only 11 days out of 180) is probably to be ascribed to the presence of synoptic disturbances, with non-uniform geostrophic wind and widespread cloud. Thus, it may be fairly confidently predicted that, in the absence of synoptic-scale disturbances and widespread cloud over the Peninsula, a Gulf bore will be observable in October somewhere in the morning glory zone, provided u_g lies within the above limits. This conclusion neglects the effect of v_g, which, if positive (as it almost always is on undisturbed days), tends to increase effective u_g.

Concerning the model

Surface fluxes

It is desirable to judge whether the modelled fluxes of heat and momentum at the land and sea surfaces are in reasonable agreement with what is known for such an area as the Peninsula and the sea on either side, for it is essentially the horizontal variation of the sensible heat flux which provides the available potential energy which drives the sea-breezes and ultimately the bores to be investigated. Sensible heat fluxes are normally much greater over land during the day than over the sea. The modelling is based largely on what was learned from the Wangara experiment at latitude 34.5°S.

The fluxes have been measured over land during the Koorin expedition (Clarke and Brook (eds) 1979) at a location not greatly dissimilar from Cape York in regard to latitude and vegetative cover, but in winter (July-August) rather than in October, when the solar elevation is higher and the heating greater. During Koorin, the geostrophic wind varied between 5.0 and 18.0 m s^{-1} at midday, with a mean of 9.6 ± 3.2 m s^{-1}. The greatest measured heat flux was 372 Wm^{-2} at 1215, day 28.

The numerical model was run in a one-dimensional mode, with geostrophic wind 9.6 m s^{-1}, every other determinant having the values used in the sea-breeze experiments described above. A few of the fluxes computed by the model are compared with fluxes measured during Koorin in Table 5. Here $\bar{H}_k$ by day is the mean of the daily maximum measured sensible heat flux on nearly cloudless days, $\bar{E}_k$ the same for latent heat flux, $\bar{\tau}_k$ the surface stress; while at night H and τ are so small and difficult to measure that there are many blanks in the record, and no data at all for E. (The largest fluxes between 2300 and 0400 hr have been used for estimating averages, and the number of days used to obtain averages is denoted by 'n'.) Modelled values of the fluxes are subscripted 'm'.

One can conclude from this table that the sensible heat flux in October on the Peninsula has probably been realistically modelled, but the surface stress has been underestimated, and hence also the viscous dissipation related thereto. The simulation could have been improved simply by using a larger value for the surface roughness parameter, z_o, more in keeping with the wooded nature of the land surface than with the grassland for which $z_o = 0.02$ m is appropriate. The latent heat flux (evaporation) has probably been overestimated, but the dynamic effects of this fault are believed to be negligible.

The most serious defect in the model from the aspect of physics is the lack of a mechanism to model cooling and heating due to radiative flux divergence within the atmosphere. This might be expected to adversely affect the quality of the modelling in very low levels, where indeed the vertical resolution which has been used is quite inadequate for such purposes.

Location of surge fronts

The exact location of modelled sea-breeze surges and

Table 5. Comparison of the surface fluxes of sensible and latent heat, and of momentum, as measured at Koorin, and as computed in the model.

Time	$\bar{H}_k$	n	H_m	$\bar{E}_k$	n	E_m	$\bar{\tau}_k$	n	τ_m
Units			watts per sq. metre				thousandths of Nm^{-2}		
Near midday	318 ± 30	24	360	193 ± 52	23	292	336 ± 250	29	239
Near midnight	-48 ± 20	16	-36	---	--	5	49 ± 38	23	31

bores is somewhat arbitrary. Three procedures have been tried: (a) the plan position of w_{max}, where w(x,z) is vertical velocity, measured on the scale of the horizontal grid, and w_{max}, is confined to levels below 2000 m; (b) the position of $(\delta p_o/\delta x)_{max}$, the maximum in surface pressure gradient; (c) the location of a transition in sign of the onshore wind component. Of these, (a) has proved the most satisfactory convention, and a quadratic fitting of the three horizontal grid values of w embracing w_{max}, shows pleasing continuity, and enables the speed of translation to be computed; (b) represents vertically integrated temperature gradient, and has been found less useful; whereas (c) may be used where u_g is negative, but not where it is positive. The temperature field is generally unsuitable as an indicator, because of its diffuseness.

Performance of the model

The numerical experiments give convincing answers to questions concerning the sequence of events during bore formation, but in some respects the results are disappointing.

Too much emphasis should not be placed on the somewhat anaemic pressure jumps associated with the bores compared with those observed, for this was remedied (see E, Fig. 9) by postulating pre-existing baroclinicity across the peninsula, and the fairly regular existence of such a temperature structure cannot, in the absence of observations, be ruled out. Certainly the weather chart and the three radiosonde flights on 24-25 October 1982 (Smith and Morton 1984) suggest that baroclinicity was strong on the occasion of this 'most massive morning glory' yet encountered in the field.

The disappointing aspect of the experiments is their inability to simulate adequately the post-bore waves which are such a dramatic feature of many morning glories in the field. They may be so strongly developed that some glories could be regarded as a succession of finite amplitude waves, rather than as a bore. Spectacular examples have been given in CSR and II. The numerical experiments of Peregrine (1966) with external bores in a liquid show that post-bore waves are not obtained with the use of a hydrostatic theory, but *are* produced when a term is included in the momentum equation for non-hydrostatic effects. The fact that we have produced small undulations of roughly the observed wavelength behind the leading bore wave with a hydrostatic model in a more complex internal bore is unexpected.

Clearly to model the undular Gulf bores in satisfactory detail would require a non-hydrostatic model, with much greater computing resources.

Lack of sufficient sharpness in the model results can be ascribed to centred differencing with insufficient resolution in both dimensions. Decay of the bore wave through upward radiation of wave energy will occur if there is stratification above the wave guide (Maslowe and Redekopp 1980), but according to Egger (1984) this should not result in rapid decay with the stratification observed at Burketown; in fact, natural bores exhibit little leakage of energy in this way. Modelled bores decay much more rapidly (Table 3). This may be due to lack of sufficient resolution, of a third dimension, or of an adequate specification of mixing through the capping inversion, but is perhaps more likely to be due to excessive dissipation resulting from the frequent (every 30 time steps) application of the Shapiro 5-point filter (Shapiro 1970). Whatever the reason, the modelled bores do lean forward (Smith and Morton 1984), do lose their energy too rapidly, and do accelerate gradually (Fig. 9).

While admitting these deficiencies, one might suppose that the neglect of horizontal (and in the case of geostrophic wind, vertical) inhomogeneities (in z_o, albedo, topography, initial fields of temperature, pressure, wind, etc.) and two-dimensionality might conspire to defeat realistic simulation of large amplitude waves: for instance, the 'clefts and lobes' of Simpson and Britter (1980) might well be instrumental in producing some of the irregularities occurring naturally in bore situations. In II we showed that the recurring tendency to produce waves of length 6 to 10 km can be roughly predicted by classical bore theory, and indeed they are by Peregrine's (1966) and Egger's (1984) highly simplified but non-hydrostatic models.

In summary, the model has succeeded in capturing the gross morphology of the bores, and little more than a hint of the post-bore disturbances, despite the high resolution used. The transition from post-bore wavelike perturbations to ordered solitary wave trains, with or without closed circulations, could hardly be expected with achievable resolution or a hydrostatic model.

Conclusions

Sea-breezes in the tropics, with onshore geostrophic wind, may be powerful, persist all night and penetrate far inland, modifying the air up to about 2 km. With offshore geostrophic winds, sea-breeze effects may be felt hundreds of kilometres to seaward. By night, sea-breezes are essentially collapsing gravity currents. Coast-parallel geostrophic wind components have relatively little effect on sea-breeze development and penetration.

The north Queensland observations and these numerical studies present a very different picture of the role of sea and land breezes from those presented for other latitudes, for example, by Neumann and Mahrer (1971), but their general validity has been amply demonstrated. The effect of pre-existing wind on sea-breeze propagation during daylight hours is found to be approximately as observed by Simpson and Britter (1980) for assisting geostrophic winds, but much less for opposing ones.

Our chief interest in this work has been to discover

what happens, in two dimensions, when two such gravity currents collide or interact on a peninsula. The investigation reveals that the collision raises cool air in a sharp upward bulge, and that from this bulge either one or two bores may propagate into the suitably conditioned stratified layer on either side of the collision site at sensibly the same speed as the erstwhile sea-breeze fronts. The bores may be undular, and maintained for some hours. The major one at least (that produced by the wind-assisted sea-breeze surge) is in a sense a combination of bore and gravity current.

The width of the peninsula, so long as it is within the limits applying on most of Cape York, has little effect on the formation and propagation rate of the major bore.

The presence of a topographical ridge on the peninsula is not necessary for these processes, although, if it is near the windward coast, the sea-breeze emerges from the anabatic flow on the steep seaward slope somewhat earlier, maintains a slight advantage throughout, and produces a slightly speedier bore than the case with no orography.

A non-zero value of the coast-parallel component of geostrophic wind has relatively little effect on the sea-breezes and consequent bore formation. Bores can be expected somewhere in the Gulf of Carpentaria region whenever relatively cloud-free conditions (in October at least) prevail, and the component of geostrophic wind normal to the axis of the Peninsula lies between about 1 and 13 m s^{-1}. Reduction of solar radiation, for example by cloud, markedly affects the strength and penetration of sea-breezes and can inhibit bore formation.

An important factor in determining the intensity of the Gulf bore is probably the baroclinicity, with temperatures in the lowest few kilometres of atmosphere increasing, on constant pressure surfaces, from the Coral Sea to the Gulf.

The effect of moist processes, such as condensation, on bore development has not been investigated. However, it can be stated that quite intense bores can occur without condensation (two such were reported in CSR).

The problem of bore behaviour in the Gulf is certainly a three-dimensional one, but the processes on Cape York, where the angle between the two opposing coasts is about 38 degrees, are evidently sufficiently near to two-dimensional that the present treatment is approximately valid. The effect of varying the orientation of the colliding sea-breezes could be investigated in a three-dimensional model, with sufficient computing resources.

The evidence to hand suggests that the morning glories coming from a southerly direction at such places as Burketown have a similar origin to those coming from the east, but the stronger gravity current is in this case a southern cold front or surge, which, at Mount Isa, is often almost indistinguishable from a sea-breeze front.

This work has obvious implications for research on 'cool changes' in southern Australia. It also lays a foundation for the investigation of the deep convective lines in the Gulf of Carpentaria described by Neal et al. (1973), and possibly of the severe storms affecting the coasts of the Northern Territory during east wind regimes.

Acknowledgments

Thanks are due to the University of Melbourne, and especially to its Meteorology Department, for the extensive use of its computing and other facilities. Gratitude is owed to D. R. Christie, J. R. Garratt, and R. K. Smith for reading the manuscript.

References

Admiralty, Naval Meteorological Branch. 1944. Tropical land and sea breezes. Branch Memo. 126/44 (HM 332/39).

Christie, D. R., Muirhead, K. J. and Hales, A. L. 1979. Intrusive density flows in the lower troposphere: a source of atmospheric solitons. *J. geophys. Res., 84,* 4959-70.

Christie, D. R. and Muirhead, K. J. 1983. Solitary waves: a hazard to aircraft operating at low altitudes. *Aust. Met. Mag., 31,* 97-110.

Clarke, R. H. 1961. The meso-structure of dry cold fronts over featureless terrain, *J. Met., 18,* 715-35.

Clarke, R. H. 1965. Horizontal mesoscale vortices in the atmosphere. *Aust. Met. Mag., 50,* 1-25.

Clarke, R. H. 1972. The morning glory: an atmospheric hydraulic jump. *Jnl appl. Met., 11,* 304-11.

Clarke, R. H. 1983a. Fair weather nocturnal inland wind surges and atmospheric bores. Part I. Nocturnal wind surges. *Aust. Met. Mag., 31,* 133-45.

Clarke, R. H. 1983b. Internal atmospheric bores in northern Australia. *Aust. Met. Mag., 31,* 147-60. (See Corrigenda *Aust. Met. Mag., 32,* 53).

Clarke, R. H. 1985. Geostrophic wind over Cape York Peninsula and pressure jumps around the Gulf of Carpentaria. *Aust. Met. Mag., 33* (in press).

Clarke, R. H. and Brook, R. R. (eds) 1979. The Koorin expedition: atmospheric boundary layer data over tropical savannah land. *Met. Summary,* Bur. Met., Australia, 359 pp.

Clarke, R. H., Smith, R. K. and Reid, D. G. 1981. The morning glory of the Gulf of Carpentaria: an atmospheric undular bore. *Mon. Weath. Rev., 109,* 1726-50.

Egger, J. 1984. On the theory of the morning glory. *Beit. zur Phys. der Atmos., 57,* 123-34.

Garratt, J. R., Physick, W. L. and Troup, A. J. 1984. The Australian summertime cool change. II Mesoscale aspects. *Mon. Weath. Rev.* (in press).

Maslowe, S. A. and Redekopp, I. G. 1980. Long non-linear waves in stratified shear flows. *J. Fluid Mech., 101,* 321-48.

Maxworthy, T. 1980. On the formation of non-linear internal waves from the gravitational collapse of mixed regions in two and three dimensions. *J. Fluid Mech., 96,* 47-64.

Neal, A. B. and Butterworth, I. J. 1973. The recurring cloud line in the Gulf of Carpentaria. *Working Paper 163,* Bur. Met., Australia, 20 pp.

Neal, A. B., Butterworth, I. J. and Murphy, K. M. 1977. The morning glory. *Tech. Report 23,* Bur. Met., Australia, 19 pp.

Neumann, J. and Mahrer, Y. 1971. A general study of land and sea-breeze circulation. *J. Atmos. Sci., 28,* 532-42.

Pearson, R. A. 1973. Properties of the sea-breeze front as shown by a numerical model. *J. Atmos. Sci., 30,* 1050-60.

Pearson, R. A., Carboni, G. and Brusasca, G. 1983. The sea-breeze with mean flow. *Q. Jl R. met. Soc., 109,* 809-30.

Peregrine, D. H. 1966. Calculation on the development of an undular bore. *J. Fluid Mech., 25,* 321-30.

Shapiro, R. 1970. Smoothing, filtering and boundary effects. *Rev. Geophys. Space Phys., 8,* 359-87.

Simpson, J. E. and Britter, R. E. 1980. A laboratory model of an atmospheric meso-front. *Q. J1 R. met. Soc., 106,* 485-500.

Simpson, J. E., Mansfield, D. A. and Milford, J. R. 1977. Inland penetration of sea-breeze fronts. *Q. J1 R. met. Soc., 103,* 47-76.

Smith, R. K., Crook, N. and Roff, G. 1982. The morning glory: an extraordinary atmospheric undular bore. *Q. J1 R. met. Soc., 108,* 937-56.

Smith, R. K. and Morton, B. R. 1984. An observational study of northeasterly 'morning glory' wind surges. *Aust. Met. Mag., 32,* 155-75.